



Audio Engineering Society

Convention Paper 7378

Presented at the 124th Convention
2008 May 17–20 Amsterdam, The Netherlands

The papers at this Convention have been selected on the basis of a submitted abstract and extended precis that have been peer reviewed by at least two qualified anonymous reviewers. This convention paper has been reproduced from the author's advance manuscript, without editing, corrections, or consideration by the Review Board. The AES takes no responsibility for the contents. Additional papers may be obtained by sending request and remittance to Audio Engineering Society, 60 East 42nd Street, New York, New York 10165-2520, USA; also see www.aes.org. All rights reserved. Reproduction of this paper, or any portion thereof, is not permitted without direct permission from the Journal of the Audio Engineering Society.

Focusing of Virtual Sound Sources in Higher Order Ambisonics

Jens Ahrens and Sascha Spors

Deutsche Telekom Laboratories, Technische Universität Berlin, Ernst-Reuter-Platz 7, 10587 Berlin, Germany

Correspondence should be addressed to Jens Ahrens (jens.ahrens@telekom.de)

ABSTRACT

Higher order Ambisonics (HOA) is an approach to the physical (re-)synthesis of a given wave field. It is based on the orthogonal expansion of the involved wave fields formulated for interior problems. This implies that HOA is per se only capable of recreating the wave field generated by events outside the listening area. When a virtual source is intended to be reproduced inside the listening area, strong artifacts arise in certain listening positions. These artifacts can be significantly reduced when a wave field with a focus point is reproduced instead of a virtual source. However, the reproduced wave field only coincides with that of the virtual source in one half-space defined by the location and nominal orientation of the focus point. The wave field in the other half-space converges towards the focus point.

1. INTRODUCTION

Higher order Ambisonics (HOA) is a sound reproduction technique that employs a large number of loudspeakers to physically recreate a wave field in a specific listening area. Since the so-called near-field correction has been introduced in [1], accurate versatile reproduction is possible. The desired wave field is typically described via its spherical harmonics expansion coefficients [1, 2]. These can be yielded either from appropriate microphone array recordings [3] (data-based reproduction) or virtual sound scenes may be composed of virtual sound sources

whose spherical harmonics expansion coefficients are derived from analytical source models (model-based reproduction). In this paper, we will concentrate on the latter case.

Besides plane waves, the virtual sound sources are traditionally modeled as monopole sources and are typically located outside the listening area. Although approaches for the reproduction of complex sources have been presented recently [4, 5], we will focus on the investigation of virtual monopole sources for simplicity. The extension of the presented approach to complex sources is straightfor-

ward and a general guideline is given.

Due to reasons of causality, it is not possible to reproduce virtual sound sources inside the listening area without artifacts, no matter which reproduction method is employed. The wave field of a virtual source inside the listening area can only be recreated maximally in one half-space defined by the location of the virtual source and the location of the loudspeakers. In the other half-space the reproduced wave field converges towards the location of the virtual source. The wave field simply travels into the wrong direction there. The reproduction of such a focused wave field is referred to as reproduction of a *focused virtual source* respectively a *focused source*. In the context of wave field synthesis (WFS), an alternative spatial reproduction approach, the time-reversal principle has been exploited to implement the reproduction of focused virtual sources [6].

One proceeds as follows: First, a virtual source is created at the position of the intended focused source but its radiated wave field is recreated behind the loudspeaker array. Then, the driving functions deriving the loudspeaker driving signals from the source input signal are time reversed, i.e. delays become anticipations. This results in a wave field that converges towards the location of the virtual source and then diverges and makes up the desired wave field.

This principle can not be adopted straightforwardly to HOA since contrary to WFS, the listening area is always surrounded by loudspeakers which all contribute at any time to the reproduced wave field. If the time of the driving functions is reversed, in any location inside the listening area there will be both, a diverging part of the wave field (the desired part) as well as a converging (unwanted) part.

As discussed in the literature [1], the conventional Ambisonics formulation does enable to partly reproduce the wave field of a virtual source which is positioned inside the listening area. However, only in a small area determined by the virtual source's location, the wave fields emitted by the loudspeakers interfere such that the desired wave field emerges. Outside this area strong artifacts arise.

In order to minimize artifacts, we propose to explicitly model the desired reproduced wave field as converging in one half-space and diverging in the other half-space. In the remainder, we refer to the latter as *target half-space*. The boundary between the

two half-spaces can then be freely rotated around the focus point. Note that a converging wave field is essentially a time-reversed diverging one.

The typical Ambisonics approach is based on the assumption of a finite number of discrete loudspeakers whose emitted wave fields superpose to an approximation of the desired one. Typically, numerical algorithms are employed to find the appropriate loudspeaker driving signals. In order to allow for an analytical treatment of the subject, we will model a continuous secondary source distribution as recently presented by the authors [7]. The theoretical basis of the presented formulation is the so-called simple source approach [8] which has gained only little attention in conjunction with spatial audio reproduction so far.

Nomenclature In the remainder of this paper, we will assume that the near-field correction is included in the Ambisonics approach as described in section 2. Thus, when we speak of Ambisonics we implicitly mean near-field corrected higher order Ambisonics (NFC-HOA).

The following conventions are used: For scalar variables, lower case denotes the time domain, upper case the temporal frequency domain. Vectors are denoted by lower case boldface. The descriptions in this paper are restricted to two-dimensional reproduction which means in this context that an observed sound field is independent from one of the spatial coordinates, i.e. $P(x, y, z, \omega) = P(x, y, \omega)$. Confer also to section 2.2.

The two-dimensional position vector in Cartesian coordinates is given as $\mathbf{x} = [x \ y]^T$. The Cartesian coordinates are linked to the polar coordinates via $x = r \cos \alpha$ and $y = r \sin \alpha$. Confer to figure 1.

The acoustic wavenumber is denoted by k . It is related to the temporal frequency by $k^2 = \left(\frac{\omega}{c}\right)^2$ with ω being the radial frequency and c the speed of sound. Outgoing monochromatic plane and cylindrical waves are denoted by $e^{-j\frac{\omega}{c}r \cos(\theta_{pw} - \alpha)}$ and $H_0^{(2)}\left(\frac{\omega}{c}r\right)$ respectively, with θ_{pw} being the propagation direction of the plane wave.

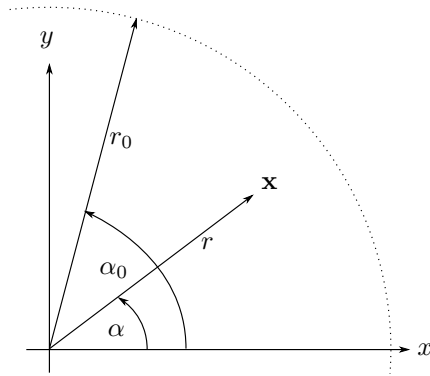


Fig. 1: The coordinate system used in this paper. The dashed line indicates the secondary source distribution.

2. THE AMBISONICS APPROACH

2.1. General Outline

In the basic three-dimensional Ambisonics approach, the loudspeakers of the respective reproduction system are located on a sphere around the listening area. Both the desired wave field as well as the sound fields emitted by the loudspeakers are expanded into series of orthogonal basis functions [9, 2]. More recent Ambisonics approaches are typically referred to as *higher order Ambisonics*. However, the term *higher order* is rather a historical rudiment. It simply emphasizes the fact that the expansions are not restricted to low (e.g. 0 or 1) expansion orders. The main motivation for concentrating on low orders is the fact that sound field recording techniques are limited to very low orders.

In this paper, we describe a general theoretical framework whose basic formulation does not take practical limitations a priori into account. We therefore waive the attribute *higher order* and implicitly speak of what is termed higher order Ambisonics, whenever we use the term Ambisonics.

The expansion of the involved wave fields into spatial basis functions allows for a mode matching procedure which leads to an equation system that is solved for the optimal loudspeaker driving signals. These drive the loudspeakers such that their superposed wave fields best approximate the desired one

in a given sense:

$$P(\mathbf{x}, \omega) = \sum_{n=0}^{N-1} D(\mathbf{x}_n, \omega) \cdot G(\mathbf{x} - \mathbf{x}_n, \omega), \quad (1)$$

where $P(\mathbf{x}, \omega)$ denotes the desired wave field, $D(\mathbf{x}_n, \omega)$ the driving signal of the loudspeaker located at the position $\mathbf{x}_n = r_0 \cdot [\cos \alpha_n \sin \alpha_n]^T$ on the sphere, and $G(\mathbf{x} - \mathbf{x}_n, \omega)$ its spatio-temporal transfer function. Typically, numerical algorithms are employed to find the appropriate loudspeaker driving signals. These algorithms tend to be computationally costly and only little insight into the properties of the actual reproduced wave-field is gained.

The Ambisonics approach is usually divided into an encoding and a decoding stage to allow for storing and transmission of content independently from the loudspeaker setup. For ease of illustration we will skip the encoding/decoding procedure and directly derive the loudspeaker driving signals from the initial virtual wave field description. The extension of the present approach to the spatial encoding and decoding of wave fields is straightforward.

2.2. Two-Dimensional Continuous Formulation

As stated in section 1, we limit our derivations to two-dimensional reproduction for convenience. In order to fulfill the requirements of the simple source approach and therefore for artifact-free reproduction, we have to assume a continuous circular distribution of secondary line sources positioned perpendicular to the target plane (the listening plane) [8]. Our approach is therefore not directly implementable since loudspeakers exhibiting the properties of line sources are commonly not available. Real-world implementation usually employ loudspeakers with closed cabinets as secondary sources. The properties of these loudspeakers are more accurately modeled by point sources.

The main motivation to focus on two dimensions is to keep the mathematic formulation simple in order to illustrate the general principle of the presented approach. The extension both to three-dimensional reproduction (i.e. spherical arrays of secondary point sources) and to two-dimensional reproduction employing circular arrangements of secondary point sources is straightforward and can be found in [7].

The formulation of the Ambisonics reproduction equation (1) considering the above mentioned as-

sumptions reads

$$P(\mathbf{x}, \omega) = \int_0^{2\pi} D(\alpha_0, \omega) G_{2D}(\mathbf{x} - \mathbf{x}_0, \omega) r_0 d\alpha_0, \quad (2)$$

where $\mathbf{x}_0 = r_0 \cdot [\cos \alpha_0 \ \sin \alpha_0]^T$. The two-dimensional free-field Green's function $G_{2D}(\mathbf{x} - \mathbf{x}_0, \omega)$ representing the spatio-temporal transfer function of a secondary source at position \mathbf{x}_0 is then the zeroth order Hankel function of second kind $H_0^{(2)}\left(\frac{\omega}{c} |\mathbf{x} - \mathbf{x}_0|\right)$ [8].

Equation (2) constitutes a circular convolution and therefore the convolution theorem

$$\hat{P}_\nu(r, \omega) = 2\pi r_0 \hat{D}_\nu(\omega) \hat{G}_\nu(r, \omega) \quad (3)$$

applies [10]. $\hat{P}_\nu(r, \omega)$, $\hat{D}_\nu(\omega)$, and $\hat{G}_\nu(r, \omega)$ denote the Fourier series expansion coefficients of $P(\mathbf{x}, \omega)$, $D(\alpha, \omega)$, and $G_{2D}(\mathbf{x} - [r_0 \ 0]^T)$ ¹.

The Fourier series expansion coefficients $\hat{F}_\nu(r, \omega)$ of a two-dimensional wave field $F(\mathbf{x}, \omega)$ can be obtained via [8]

$$\hat{F}_\nu(r, \omega) = \frac{1}{2\pi} \int_0^{2\pi} F(\mathbf{x}, \omega) e^{-j\nu\alpha} d\alpha. \quad (4)$$

The wave field $F(\mathbf{x}, \omega)$ can then be synthesized as

$$F(\mathbf{x}, \omega) = \sum_{\nu=-\infty}^{\infty} \hat{F}_\nu(r, \omega) e^{j\nu\alpha}. \quad (5)$$

For propagating wave fields the coefficients $\hat{F}_\nu(r, \omega)$ can be decomposed as

$$\hat{F}_\nu(r, \omega) = \check{F}_\nu(\omega) J_\nu\left(\frac{\omega}{c} r\right), \quad (6)$$

whereby $J_\nu(\cdot)$ denotes the ν -th order Bessel function [8].

From (3) we can deduct that

$$\hat{D}_\nu(\omega) = \frac{1}{2\pi r_0} \frac{\hat{P}_\nu(r, \omega)}{\hat{G}_\nu(r, \omega)}. \quad (7)$$

Introducing the explicit formulation for the Fourier series expansion coefficients (equation (6)), we find

¹Note that the coefficients $\hat{G}_\nu(r, \omega)$ as used throughout this paper assume that the secondary source is situated at the position ($r = r_0, \alpha = 0$) and is orientated towards the coordinate origin.

that the radius r appears both in the numerator as well as in the denominator in the factor $J_\nu\left(\frac{\omega}{c} r\right)$ which cancels out for all r where $J_\nu\left(\frac{\omega}{c} r\right) \neq 0$. Whenever $J_\nu\left(\frac{\omega}{c} r\right) = 0$, de l'Hôpital's rule [11] can be applied to proof that $J_\nu\left(\frac{\omega}{c} r\right)$ and thus r also cancel out in these cases.

Combining (7) and (5) finally yields the driving function $D(\alpha, \omega)$ for a secondary source situated at position \mathbf{x}_0 reproducing a desired wave field with expansion coefficients $\hat{P}_\nu(\omega)$ reading

$$D(\alpha, \omega) = \frac{1}{2\pi r_0} \sum_{\nu=-\infty}^{\infty} \frac{\check{P}_\nu(\omega)}{\check{G}_\nu(\omega)} e^{j\nu\alpha}, \quad (8)$$

whereby we omitted the index 0 in α_0 for convenience. Note that $D(\alpha, \omega)$ is independent from the receiver position.

The coefficients $\hat{G}_\nu(r, \omega)$ respectively $\check{G}_\nu(\omega)$ describe the spatial transfer function of the employed secondary sources. These need not necessarily be modeled as monopole line sources. In principle, any two-dimensional secondary source transfer function that does not exhibit zeros can be handled in the presented approach. However, the directivity characteristics have to be equal for all loudspeakers. We assume monopole line sources in the remainder of this paper for convenience.

Equation (8) can be verified by inserting it into (2). After introducing the Fourier series expansion of the secondary source wave fields according to (6), exchanging the order of integration and summation, and exploitation of the orthogonality of the circular harmonics $e^{j\nu\alpha}$ [8] one arrives at the Fourier series expansion of the desired wave field, thus proving perfect reproduction. Note however that the coefficients $\hat{P}_\nu(\omega)$ respectively $\check{G}_\nu(\omega)$ are typically derived from interior expansions. This implies that (8) is generally only valid inside the secondary source distribution.

2.3. Conventional Reproduction of Virtual Sound Sources

In this section, we briefly outline the properties of the conventional approach of reproducing virtual sound sources. Exemplarily, we assume the virtual source as well as the secondary sources to be monopole line sources.

The wave field $S(\mathbf{x} - \mathbf{x}_s, \omega)$ of such a monopole line

source situated at position \mathbf{x}_s reads [8, 12]

$$\begin{aligned} S(\mathbf{x} - \mathbf{x}_s, \omega) &= H_0^{(2)}\left(\frac{\omega}{c}|\mathbf{x} - \mathbf{x}_s|\right) = \\ &= \sum_{\nu=-\infty}^{\infty} J_{\nu}\left(\frac{\omega}{c}r\right) \underbrace{H_{\nu}^{(2)}\left(\frac{\omega}{c}r_s\right) e^{-j\nu\alpha_s} e^{j\nu\alpha}}_{\tilde{S}_{\nu}(\omega)}. \end{aligned} \quad (9)$$

Note that (9) only holds true for $|\mathbf{x}| < |\mathbf{x}_s|$.

Introducing (9) for the wave fields of the secondary sources as well as for the wave field of the virtual source into (8) yields the driving function $D_{\text{conv}}(\alpha, \omega)$ for a continuous circular distribution of secondary monopole line source reproducing a virtual monopole line source at position \mathbf{x}_s . Explicitly,

$$D_{\text{conv}}(\alpha, \omega) = \frac{1}{2\pi r_0} \sum_{\nu=-\infty}^{\infty} \frac{H_{\nu}^{(2)}\left(\frac{\omega}{c}r_s\right)}{H_{\nu}^{(2)}\left(\frac{\omega}{c}r_0\right)} e^{j\nu(\alpha - \alpha_s)}. \quad (10)$$

As long as $r_s > r_0$, thus as long as the virtual line source is located outside the listening area, the line source's wave field can be perfectly reproduced inside the listening area. However, when $r_s < r_0$ the reproduced wave field only coincides with the desired one inside the disc with radius r_s . Outside this disc strong artifacts arise, most notably a strong boost of bass frequencies [1]. Thus, the closer the virtual source is to the coordinate origin, the smaller is the disc on which the desired wave field is reproduced. Confer to figure 2 for an illustration.

In the following sections, we derive a strategy to minimize the artifacts that the reproduction of virtual sound sources positioned inside the listening area implies.

2.4. Modeling of a Wave Field Exhibiting a Focus Point

In this section, we derive a mathematical formulation for the wave field which we intend to reproduce, i.e. a wave field converging in one half-space towards a focus point and diverging into the target half-space. In the target half-space, we want the diverging wave field to resemble that of a virtual sound source located at the position of the focus point. For convenience, we choose this virtual source to be a monopole line source.

The wave field of a such a monopole line source situated at the origin of the coordinate system reads

$$S(\mathbf{x}, \omega) = H_0^{(2)}\left(\frac{\omega}{c}r\right). \quad (11)$$

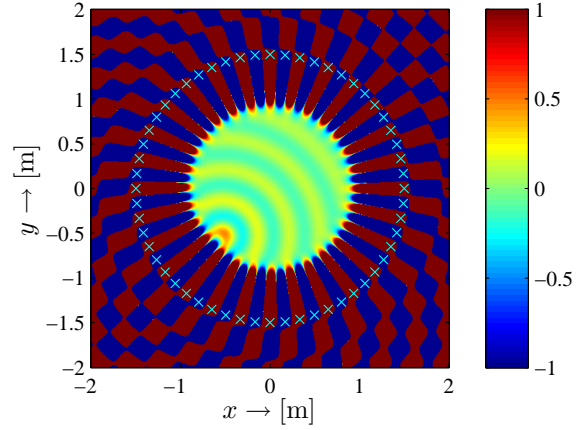


Fig. 2: Wave field generated by a circular setup of 56 secondary line sources with a radius of $r_0 = 1.5$ m reproducing a virtual line source at position ($r_s = 0.75$ m, $\alpha_s = -\frac{3\pi}{4}$). The emitted frequency is $f = 1000$ Hz. The values of the sound pressure are clipped as indicated by the colorbars. The marks indicate the positions of the secondary sources.

The spatial spectrum $\tilde{S}(\mathbf{k}, \omega)$ of $S(\mathbf{x}, \omega)$ can be obtained via a spatial Fourier transform yielding [13]

$$\tilde{S}(\mathbf{k}, \omega) = \frac{j}{(k)^2 - \left(\frac{\omega}{c}\right)^2} + \frac{1}{k} \delta\left(k - \frac{\omega}{c}\right), \quad (12)$$

whereby $\delta(\cdot)$ denotes the Dirac delta function [10]. The spatial spectrum $\tilde{S}(\mathbf{k}, \omega)$ of a wave field $S(\mathbf{x}, \omega)$ describes a spatial composition of $S(\mathbf{x}, \omega)$.

The first addend in (12) describes the evanescent part [14], the second added the propagating part [14]. We will ignore the evanescent part in the remainder of this paper.

An inverse spatial Fourier transform of (12) would yield the temporal spectrum $S_{\text{prop}}(\mathbf{x}, \omega)$ of the propagating part of $S(\mathbf{x}, \omega)$. However, due to the causality restrictions mentioned in section 1, $S_{\text{prop}}(\mathbf{x}, \omega)$ can only be reproduced in one half-space. We therefore perform the inverse Fourier transform exclusively over the half-space where we want to reproduce $S_{\text{prop}}(\mathbf{x}, \omega)$ (the target half-space). For convenience, we choose the half-space bounded by the y -axis and including the positive x -axis as target half-space. The inverse spatial Fourier transform of the propagating part of (12) over the target-half space

reads then

$$P(\mathbf{x}, \omega) = \frac{1}{4\pi^2} \int_0^\infty \int_{-\frac{\pi}{2}}^{\frac{\pi}{2}} \frac{\delta(k - \frac{\omega}{c})}{k} e^{-jk r \cos(\theta - \alpha)} d\theta dk . \quad (13)$$

Exploiting the sifting property of the Dirac delta function [10], the double-integral in (13) can be simplified to an integral from $-\frac{\pi}{2}$ to $\frac{\pi}{2}$ along a semicircle of radius $\frac{\omega}{c}$ reading

$$P(\mathbf{x}, \omega) = \frac{1}{4\pi^2} \int_{-\frac{\pi}{2}}^{\frac{\pi}{2}} e^{-j\frac{\omega}{c} r \cos(\theta - \alpha)} d\theta . \quad (14)$$

Introducing the Jacobi-Anger expansion [15]

$$e^{-j\frac{\omega}{c} r \cos(\theta - \alpha)} = \sum_{\eta=-\infty}^{\infty} j^{-\eta} J_\eta \left(\frac{\omega}{c} r \right) e^{j\eta(\alpha - \theta)} \quad (15)$$

into (13) yields the temporal spectrum of a wave field diverging from the origin of the coordinate system into the target half-space reading

$$\begin{aligned} P(\mathbf{x}, \omega) &= \frac{1}{4\pi^2} \int_{-\frac{\pi}{2}}^{\frac{\pi}{2}} \sum_{\eta=-\infty}^{\infty} j^{-\eta} J_\eta \left(\frac{\omega}{c} r \right) e^{j\eta(\alpha - \theta)} d\theta = \\ &= \sum_{\eta=-\infty}^{\infty} \frac{j^{-\eta}}{4\pi} \text{sinc} \left(\frac{\eta}{2} \right) J_\eta \left(\frac{\omega}{c} r \right) e^{j\eta\alpha} , \quad (16) \end{aligned}$$

whereby $\text{sinc}(x) = \frac{\sin(\pi x)}{\pi x}$ [10]. Note that $P(\mathbf{x}, \omega)$ converges towards the coordinate origin in the other half-space.

In order to rotate the target half-space around the coordinate origin (the focus point of $P(\mathbf{x}, \omega)$), we introduce the nominal orientation $\alpha_{\mathbf{n}}$ of the focus point (confer to figure 3) into (16) as

$$P(\mathbf{x}, \omega) = \sum_{\eta=-\infty}^{\infty} \frac{j^{-\eta}}{4\pi} \text{sinc} \left(\frac{\eta}{2} \right) J_\eta \left(\frac{\omega}{c} r \right) e^{j\eta(\alpha - \alpha_{\mathbf{n}})} . \quad (17)$$

$\alpha_{\mathbf{n}}$ denotes the direction of the normal on the half-space boundary pointing into the target half-space. Equation (17) reformulated for arbitrary positions \mathbf{x}_{foc} of the focus point reads

$$\begin{aligned} P(\mathbf{x}, \omega) &= \sum_{\eta=-\infty}^{\infty} \frac{j^{-\eta}}{4\pi} \text{sinc} \left(\frac{\eta}{2} \right) J_\eta \left(\frac{\omega}{c} r'(\mathbf{x}) \right) \times \\ &\quad \times e^{j\eta(\alpha'(\mathbf{x}) - \alpha_{\mathbf{n}})} , \quad (18) \end{aligned}$$

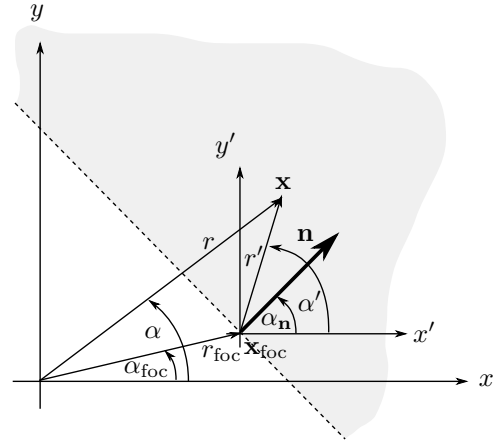


Fig. 3: Definition of the local coordinate system and the nominal orientation of the focus point situated at position \mathbf{x}_{foc} . The normal vector \mathbf{n} points into the target half-space which is indicated by the grey-shaded area and bounded by the dashed line.

whereby the prime indicates that the respective quantity belongs to the local coordinate system with origin at \mathbf{x}_{foc} whose axes are parallel to those of the global coordinate system (confer to figure 3). However, in order to yield the coefficients $\check{P}_\eta(\omega)$ (equation (6)) which the driving function (8) incorporates, we have to expand (18) around the origin of the global coordinate system. We therefore introduce the addition theorem for cylinder harmonics [12]

$$\begin{aligned} J_\eta \left(\frac{\omega}{c} r' \right) e^{j\eta\alpha'} &= \\ &= \sum_{\nu=-\infty}^{\infty} J_\nu \left(\frac{\omega}{c} r \right) J_{\nu-\eta} \left(\frac{\omega}{c} r_{\text{foc}} \right) \times \\ &\quad \times e^{-j(\nu-\eta)\alpha_{\text{foc}}} e^{j\nu\alpha} \quad (19) \end{aligned}$$

into (18) finally yielding

$$\begin{aligned} P(\mathbf{x}, \omega) &= \sum_{\nu=-\infty}^{\infty} \sum_{\eta=-\infty}^{\infty} \frac{j^{-\eta}}{4\pi} \text{sinc} \left(\frac{\eta}{2} \right) e^{-j\eta\alpha_{\mathbf{n}}} \times \\ &\quad \times J_\nu \left(\frac{\omega}{c} r \right) J_{\nu-\eta} \left(\frac{\omega}{c} r_{\text{foc}} \right) e^{-j(\nu-\eta)\alpha_{\text{foc}}} e^{j\nu\alpha} . \quad (20) \end{aligned}$$

for the wave field $P(\mathbf{x}, \omega)$ focused at the point $\mathbf{x}_{\text{foc}} = r_{\text{foc}} \cdot [\cos \alpha_{\text{foc}} \sin \alpha_{\text{foc}}]^T$ and with nominal orientation $\alpha_{\mathbf{n}}$.

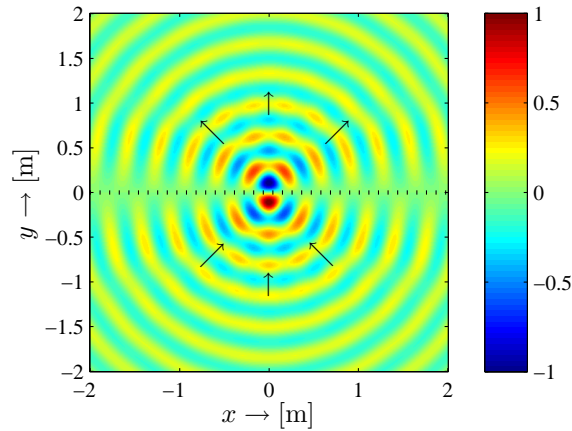


Fig. 4: Wave field $P(\mathbf{x}, \omega)$ exhibiting a focus point at the coordinate origin. The nominal orientation of the focus point is $\alpha_{\mathbf{n}} = \frac{\pi}{2}$. The expansion orders are limited to the interval $[-20; 20]$. The dashed line indicates the boundary of the target half-space. The arrows indicate the local propagation direction. The emitted frequency is $f = 1000$ Hz.

The wave field described by equation (20) is illustrated in figure 4. It depicts a wave field with a focus point in the coordinate origin and nominal orientation $\alpha_{\mathbf{n}} = \frac{\pi}{2}$. The wave field converges in the half-space including the negative y -axis and diverges in the half-space including the positive y -axis (the target half-space).

Note that the expansion orders of $P(\mathbf{x}, \omega)$ are limited to the interval $[-20; 20]$. However, even a radical extension of the angular bandwidth does not significantly reduce the distortions in the wave fronts. We assume that these distortions are artifacts due to the limitation of the aperture introduced in equation (13) (*Gibbs phenomenon* [16]). Note that the choice of the aperture angle in (13) as well as weighting of angular spatial spectrum provide potential to reduce these artifacts.

Note also that although not apparent in figure 4, there is no phase discontinuity in the focus point as opposed to focus points generated in WFS by applying the pure time-reversal approach (confer to section 1).

2.5. Focusing Virtual Complex Sources

In order to reproduce a focused virtual complex source (i.e. a directional or spatially extended one, confer to [4, 5]), the procedure outlined in section 2.4 can be straightforwardly applied. The inverse Fourier transform over the target half-space of the far-field radiation characteristics of the complex source (confer to (13)) leads to the desired formulation of the corresponding focused wave field.

3. RESULTS

From equation (20) we can extract the expansion coefficients $\check{P}_{\nu}(\omega)$ (confer to (6)) of the focused wave field reading

$$\check{P}_{\nu}(\omega) = \sum_{\eta=-\infty}^{\infty} \frac{j^{-\eta}}{4\pi} \text{sinc}\left(\frac{\eta}{2}\right) e^{-j\eta\alpha_{\mathbf{n}}} \times J_{\nu-\eta}\left(\frac{\omega}{c}r_{\text{foc}}\right) e^{-j(\nu-\eta)\alpha_{\text{foc}}}. \quad (21)$$

In order to reproduce a wave field given by (20) with a circular distribution of loudspeakers, the coefficients $\check{P}_{\nu}(\omega)$ have to be incorporated into the driving function equation (8). When the secondary source array is a continuous distribution of secondary line sources perpendicular to the listening plane, the desired wave field is perfectly recreated inside the listening plane as derived in section 2.2. The detailed analysis of the properties of the wave field reproduced by a setup of discrete loudspeakers is beyond the scope of this paper.

To get a first impression of the properties of the presented approach, we provide numerical simulations in figure 5. Figure 5 depicts wave fields generated by a circular setup of 56 secondary monopole line sources with a radius of $r_0 = 1.5$ m reproducing a focused monopole line source at position ($r_{\text{foc}} = 0.75$ m, $\alpha_{\text{foc}} = -\frac{3\pi}{4}$) with different nominal orientations $\alpha_{\mathbf{n}}$. The emitted frequency is $f = 1000$ Hz.

As noted in section 2.4, the distortions of the wave fronts apparent in figure 5 are suspected to be unavoidable due to a limitation of the aperture. Figure 5 illustrates the freedom that the arbitrary choice of the nominal orientation $\alpha_{\mathbf{n}}$ of the focus point enables. Knowledge of the listeners' positions can be exploited to orientate the virtual source such that the target half-space covers as many listeners as possible.

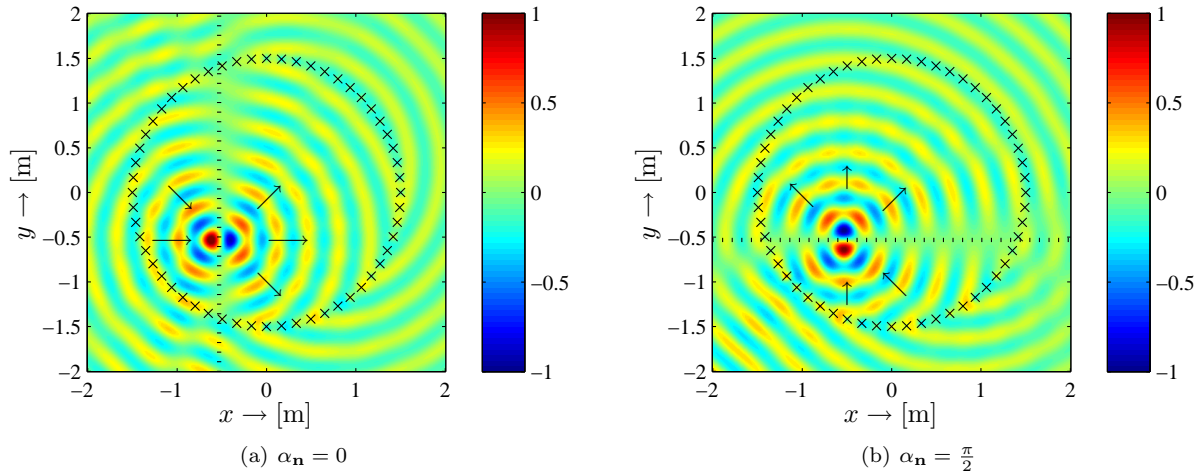


Fig. 5: Wave field generated by a circular setup of 56 secondary line sources with a radius of $r_0 = 1.5$ m reproducing a focus point at position ($r_{\text{foc}} = 0.75$ m, $\alpha_{\text{foc}} = -\frac{3\pi}{4}$) with different nominal orientations α_n . The emitted frequency is $f = 1000$ Hz. The arrows indicate the local propagation direction of the wave field. The dashed line indicates the boundary of the target half-space. The values of the sound pressure are clipped as indicated by the colorbars. The marks indicate the positions of the secondary sources.

4. CONCLUSIONS

A basic framework for the reproduction of virtual sound sources inside the listening area (so-called *focused sources*) in higher order Ambisonics was presented. Actually, the approach does not intend to reproduce a virtual source but a wave field exhibiting a focus point at the position of the intended virtual source. In one half-space determined by position of the focus point, the reproduced wave field converges towards the focus point. In the other half-space, the target half-space, the wave field diverges and evokes the perception of a virtual source at the position of the focus point. This strategy avoids certain limitations of the conventional straightforward approach as discussed.

The target half-space may be freely rotated around the focus point. This fact enables the optimization of the reproduction for given listener positions. We presented numerical simulations of reproduced wave fields to illustrate the general properties of the proposed approach. However, a thorough analytical investigation was beyond the scope of the paper.

5. REFERENCES

[1] J. Daniel. Spatial sound encoding including

near field effect: Introducing distance coding filters and a viable, new ambisonic format. In *23rd Int. Conf., May 23–25, Copenhagen, Denmark, 2003*. Audio Engineering Society (AES).

- [2] J. Daniel. Représentation de champs acoustiques, application à la transmission et à la reproduction de scènes sonores complexes dans un contexte multimédia. PhD thesis Université Paris 6, 2001.
- [3] M.A. Poletti. Three-dimensional surround sound systems based on spherical harmonics. *Journal of the Audio Engineering Society (AES)*, 53(11):1004–1025, Nov. 2005.
- [4] J. Ahrens and S. Spors. Rendering of virtual sound sources with arbitrary directivity in higher order ambisonics. *123rd AES Conv., NY, NY, USA, 5–8 Oct., 2007*.
- [5] D. Menzies. Ambisonic synthesis of complex sources. *JAES*, 55(10):864–876, Oct. 2007.
- [6] E.N.G. Verheijen. Sound reproduction by wave field synthesis. PhD thesis, Delft University of Technology, 1997.

- [7] J. Ahrens and S. Spors. Analytical driving functions for higher order ambisonics. In *IEEE International Conference on Acoustics, Speech, and Signal Processing (ICASSP)*, Las Vegas, Nevada, March 30th–April 4th 2008.
- [8] E.G. Williams. *Fourier Acoustics: Sound Radiation and Nearfield Acoustic Holography*. Academic Press, London, 1999.
- [9] M.A. Gerzon. With-height sound reproduction. *Journal of the Audio Engineering Society (JAES)*, 21:2–10, 1973.
- [10] B. Girod, R. Rabenstein, and A. Stenger. *Signals and Systems*. J.Wiley & Sons, 2001.
- [11] E.W. Weisstein. L'Hospital's Rule. MathWorld – A Wolfram Web Resource. <http://mathworld.wolfram.com/LHospitalsRule.html>.
- [12] Milton Abramowitz and Irene A. Stegun, editors. *Handbook of Mathematical Functions*. Dover Publications Inc., New York, 1968.
- [13] Sascha Spors. Active listening room compensation for spatial sound reproduction systems. PhD thesis, University of Erlangen-Nuremberg, 2005.
- [14] S. Spors and J. Ahrens. Analysis of near-field effects of wave field synthesis using linear loudspeaker arrays. *30th Int. Conference of the AES, Saariselkä, Finland*, March 2007.
- [15] E.W. Weisstein. Jacobi-Anger Expansion. MathWorld – A Wolfram Web Resource. <http://mathworld.wolfram.com/Jacobi-AngerExpansion.html>.
- [16] E.W. Weisstein. Gibbs Phenomenon. MathWorld – A Wolfram Web Resource. <http://mathworld.wolfram.com/GibbsPhenomenon.html>.